

## Influence of chlorine on the fate of Pb and Cu during clinkerization

Bin Zhang, Anna Bogush, Jiangxiong Wei, Weiting Xu, Zhengxiang Zeng, Tongsheng Zhang, Qijun Yu, and Julia Anna Stegemann

*Energy Fuels*, **Just Accepted Manuscript** • DOI: 10.1021/acs.energyfuels.8b01111 • Publication Date (Web): 13 Jun 2018

Downloaded from <http://pubs.acs.org> on June 18, 2018

### Just Accepted

“Just Accepted” manuscripts have been peer-reviewed and accepted for publication. They are posted online prior to technical editing, formatting for publication and author proofing. The American Chemical Society provides “Just Accepted” as a service to the research community to expedite the dissemination of scientific material as soon as possible after acceptance. “Just Accepted” manuscripts appear in full in PDF format accompanied by an HTML abstract. “Just Accepted” manuscripts have been fully peer reviewed, but should not be considered the official version of record. They are citable by the Digital Object Identifier (DOI®). “Just Accepted” is an optional service offered to authors. Therefore, the “Just Accepted” Web site may not include all articles that will be published in the journal. After a manuscript is technically edited and formatted, it will be removed from the “Just Accepted” Web site and published as an ASAP article. Note that technical editing may introduce minor changes to the manuscript text and/or graphics which could affect content, and all legal disclaimers and ethical guidelines that apply to the journal pertain. ACS cannot be held responsible for errors or consequences arising from the use of information contained in these “Just Accepted” manuscripts.



## Influence of chlorine on the fate of Pb and Cu during clinkerization

Bin Zhang<sup>1</sup>, Anna Bogush<sup>2</sup>, Jiangxiong Wei<sup>1,3\*</sup>, Weiting Xu<sup>1</sup>, Zhengxiang Zeng<sup>1</sup>,

Tongsheng Zhang<sup>1,3</sup>, Qijun Yu<sup>1,3</sup>, Julia Stegemann<sup>2</sup>

<sup>1</sup>School of Materials Science and Engineering, South China University of Technology, Guangzhou 510640, Guangdong, China

<sup>2</sup>Centre for Resource Efficiency & the Environment (CREE), Department of Civil, Environmental & Geomatic Engineering (CEGE), University College London (UCL), Chadwick Building, Gower Street, London WC1E 6BT, UK

<sup>3</sup>Guangdong Low Carbon Technologies Engineering Center for Building Materials, Guangzhou 510640, Guangdong, China

### ABSTRACT

The fate of heavy metals during clinkerization is of crucial significance to the utilization of solid waste as fuels and raw materials in cement kiln producing clinker. A ternary system of clinker-heavy metal-chlorine was developed that is more coincident with the condition of co-processing of solid waste in cement kiln. The main goal of this study was to investigate the relationships among chlorine, volatilization and solidification of Cu/Pb, and mineral phases of the clinker during clinkerization. The  $\text{AlCl}_3 \cdot 6\text{H}_2\text{O}$  (chlorine source) and PbO/CuO were mixed with cement raw meal in appropriate ratios to produce co-processed clinkers. The

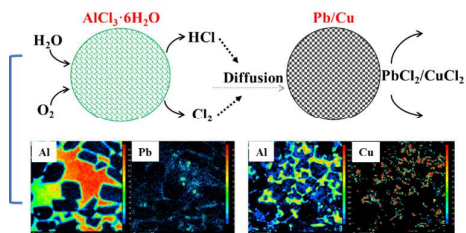
---

\* Corresponding author: [jxwei@scut.edu.cn](mailto:jxwei@scut.edu.cn), Tel.: +86 020 8711 4137

1  
2  
3  
4 23 volatilization and solidification of Pb and Cu were investigated experimentally using  
5  
6 24 a combination of atomic absorption spectrometry, electron probe micro-analysis,  
7  
8 25 scanning electron microscopy with energy-dispersive X-ray spectroscopy, optical  
9  
10  
11 26 microscope, thermogravimetric and X-ray diffraction quantitative analyses. The  
12  
13 27 volatilization ratios of Pb and Cu increased up to 46.18% and 34.04%, respectively,  
14  
15 28 with increasing  $\text{AlCl}_3 \cdot 6\text{H}_2\text{O}$  content up to 1.6%. comparing to the cement mixtures  
16  
17 29 without  $\text{AlCl}_3 \cdot 6\text{H}_2\text{O}$  addition (Pb and Cu volatilisation ratios are 49.90% and 27.21%,  
18  
19 30 respectively). Pb and Cu oxides can be transformed into Pb and Cu chlorides, that are  
20  
21 31 not stable and have high vapor pressure. Pb and Cu are mainly concentrated in the  
22  
23 32 interstitial phases of the clinker. The addition of  $\text{AlCl}_3 \cdot 6\text{H}_2\text{O}$  led to increase the  
24  
25 33 crystal size of alite and belite. X-ray diffraction quantitative analyses proved that the  
26  
27 34 content of silicate phase increased with the corresponding content of interstitial  
28  
29 35 phases decreased during clinkerization with the addition of  $\text{AlCl}_3 \cdot 6\text{H}_2\text{O}$ , that  
30  
31 36 decreased the ability of clinker to solidify Pb and Cu in the produced clinkers. This  
32  
33 37 research can help to promote understanding of the fate of heavy metals during the  
34  
35 38 cement kiln co-processing of solid wastes and meaningfully for energy conservation  
36  
37 39 and sustainable development.  
38  
39  
40  
41  
42  
43  
44

45  
46  
47 41 Key words: energy; chlorine; heavy metals; clinkerization; volatilization; mineral  
48  
49 42 phases  
50  
51  
52  
53  
54

55 44 **TOC/Abstract Art**  
56  
57  
58  
59  
60



## Synopsis

The relationships among chlorine, volatilization/solidification of Pb and Cu, and mineral phases of the cement clinker were demonstrated, which is essential for the utilization of solid waste as fuels and raw materials in cement kiln.

## 1. Introduction

The cement industry consumes around 2% of global primary energy use and produces 5-7% of anthropogenic  $\text{CO}_2$  emissions worldwide. China's cement industry accounted for more than half of the world's total cement production.<sup>1</sup> Meanwhile, China produced 3.28 billion tons of industrial solid waste, 173 million tons of municipal solid waste (MSW) and 25 million tons of sludge in 2016.<sup>2</sup> Solid wastes can be considered as secondary raw fuels and/or materials in the cement industry. The cement kiln, known to consume a large quantity of energy and raw materials, promotes to use solid waste (SW) as fuels and raw materials in replacement for traditional materials used during the manufacturing process.<sup>3-4</sup>

However, the content of chlorine and heavy metals in SW are much higher than that of in traditional raw fuels and materials (e.g., coal and limestone).<sup>5-6</sup> Previous studies carried out on heavy metal emissions from waste incineration indicated that the volatilization of heavy metals depends on the composition of the wastes, the

1  
2  
3  
4 65 physicochemical properties of heavy metals, and the compounds formed during  
5  
6 66 incineration.<sup>7-8</sup> In particular, the waste-derived chlorine significantly affects the heavy  
7  
8 67 metal emissions by the formation of volatile metallic chlorides.<sup>9-10</sup> Therefore, during  
9  
10 68 the utilization of solid waste as fuel and raw material in cement kiln, heavy metals  
11  
12 69 volatilization may be promoted by chlorine. Volatilized heavy metals can move with  
13  
14 70 flue gas to concentrate on the wall of kiln, precalciner and cyclones, and then even  
15  
16 71 exhaust into the atmosphere, which have serious effects on cement production and  
17  
18 72 environment.<sup>11-14</sup> Accordingly, understanding the influence of chlorine on the fate of  
19  
20 73 heavy metals in clinkerization is significant for the co-processing of solid wastes in  
21  
22 74 the cement kiln.

23  
24  
25  
26  
27  
28 75 Available literatures mainly focused on the effects of chlorides (such as NaCl  
29  
30 76 and KCl) on the volatilization of heavy metals during the solid wastes  
31  
32 77 incineration.<sup>15-18</sup> However, the incineration temperatures are relatively low (<1000°C)  
33  
34 78 and incineration environment and raw materials are different comparing to the cement  
35  
36 79 clinker production (T=1450°C). Additionally, cations from the chlorides such as Na<sup>+</sup>  
37  
38 80 and K<sup>+</sup> will have some effects on the process of clinkerization and then affect the  
39  
40 81 volatilization and solidification of heavy metals.<sup>19-20</sup> Besides, AlCl<sub>3</sub>·6H<sub>2</sub>O is  
41  
42 82 commonly exist in the municipal solid waste such as sewage sludge and industrial  
43  
44 83 solid waste such as red mud.<sup>17,18,21</sup> Therefore, in order to eliminate influence of  
45  
46 84 cations (such as Na<sup>+</sup> and K<sup>+</sup>) on the clinkerisation process, AlCl<sub>3</sub>·6H<sub>2</sub>O (additionally,  
47  
48 85 aluminum is one of the constituent elements of clinker) was selected as chlorine  
49  
50 86 source in this study.  
51  
52  
53  
54  
55  
56  
57  
58  
59  
60

1  
2  
3  
4 87 Pb and Cu commonly exist in the solid wastes such as Pb-Zn slag and sewage  
5  
6 88 sludge<sup>22-23</sup> that have the potential threat to volatilize and move with flue gas into the  
7  
8 89 atmosphere. Pb is one of the highly toxic heavy metals and can easily volatilize  
9  
10  
11 90 during the heat treatment of solid waste. In cement clinkering, CuO is known to act as  
12  
13 91 mineralizer because it decreases the melt temperature considerably and favours the  
14  
15 92 combination of free lime.<sup>20, 24</sup>

16  
17  
18 93 Yu *et al.*<sup>22</sup> studied the effects of chlorine on the volatilization of heavy metals  
19  
20 94 during the co-combustion of sewage sludge. Author showed that chlorine increased  
21  
22 95 the volatilization ratio of heavy metals during clinkerization. Fukuda *et al.*<sup>25</sup> focused  
23  
24 96 in a melt-differentiation mechanism to understand the crystallization behavior of  
25  
26 97 aluminates, other than the effects of chlorine on the fate of heavy metals during  
27  
28 98 clinkerization. Therefore, the binary systems of clinker-heavy metal or heavy  
29  
30 99 metal-chlorine have been investigated in previous works of co-processing of solid  
31  
32 100 waste in cement kiln. In this study, a ternary system of clinker-heavy metal-chlorine  
33  
34 101 was developed that is more coincident with the condition of co-processing of solid  
35  
36 102 waste in cement kiln. The main goal of this study was to investigate the relationships  
37  
38 103 among chlorine, volatilization and solidification of Cu/Pb, and mineral phases of the  
39  
40 104 clinker during clinkirization. The results obtained in this study can give some  
41  
42 105 suggestions to reduce the volatilization of Cu and Pb by adjusting mineral  
43  
44 106 compositions of the clinker when co-processing of chlorine-contained solid waste in  
45  
46 107 the cement kiln.

47  
48  
49  
50  
51  
52  
53  
54  
55 108

1  
2  
3  
4  
5  
6  
7  
8  
9  
10  
11  
12  
13  
14  
15  
16  
17  
18  
19  
20  
21  
22  
23  
24  
25  
26  
27  
28  
29  
30  
31  
32  
33  
34  
35  
36  
37  
38  
39  
40  
41  
42  
43  
44  
45  
46  
47  
48  
49  
50  
51  
52  
53  
54  
55  
56  
57  
58  
59  
60

109 **2. Materials and methods**

110 *2.1. Materials*

111 Cement raw materials such as limestone, clay, and iron tailing, were supplied by  
112 the Yue Bao cement plant (China). Table 1 summarizes the chemical compositions of  
113 cement raw materials determined by X-ray fluorescence (XRF) analysis.

114 **Table 1**

115 Chemical compositions of the raw materials (%).

Material	Chemical composition								
	SiO <sub>2</sub>	Al <sub>2</sub> O <sub>3</sub>	Fe <sub>2</sub> O <sub>3</sub>	CaO	MgO	SO <sub>3</sub>	P <sub>2</sub> O <sub>5</sub>	LOI	Others
Limestone	4.36	BDL	1.64	53.07	0.47	0.44	0.04	39.69	0.29
Clay	65.32	17.34	4.71	1.21	0.48	0.9	0.14	0.04	9.87
Iron tailing	34.45	4.29	30.87	26.87	0.25	0.04	0.05	0.03	3.15

116 Note: BDL – below detection limit which is 0.01%, LOI: loss on ignition.

117  
118 Table 2 summarizes the content of Pb, Cu, and Cl in the raw materials analyzed  
119 by atomic absorption spectrometry (Analytik Jena AG, Germany) after total acid  
120 digestion. Although the concentrations of Pb and Cu in clay are 49 mg/kg and 19  
121 mg/kg respectively, they are far away below the detection limit of electron probe  
122 micro-analysis (EPMA) and energy dispersive spectrometer (EDS). Therefore,  
123 exogenous heavy metals of Pb and Cu were added to the raw mixes as PbO and CuO.

124 **Table 2**

125 Concentrations of Pb, Cu, and Cl in the raw materials (mg/kg).

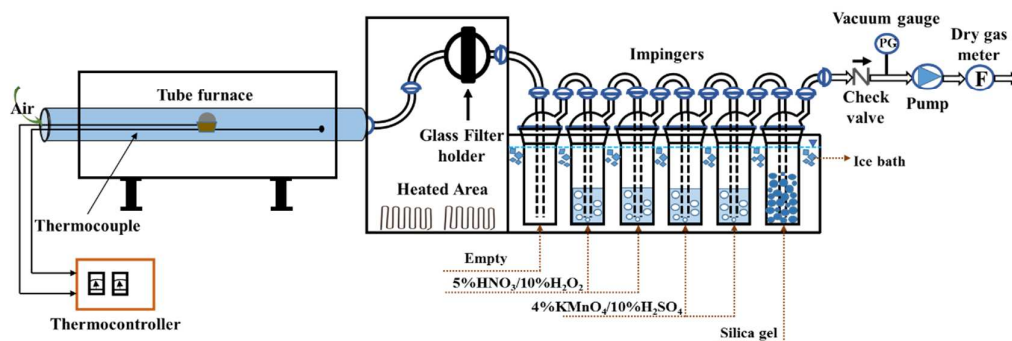
Elements	Limestone	Clay	Iron tailing
Pb	1.1	49	2.7
Cu	3.9	19	3.0
Cl	1.0	1.3	2.2

126

127 *2.2. Apparatus*

128 Figure 1 shows a laboratory apparatus used for cement clinker production. The  
129 furnace is an alundum tube with length of 120 cm and inner diameter of 7.0 cm. The  
130 temperature of heating area of the alundum tube is monitored by a thermocouple and  
131 controlled automatically. A quartz-fiber filter was set up next to the alundum tube. The  
132 filter is 99.99% effective for the removal of 0.3  $\mu\text{m}$  particles. The sampling train  
133 consisted of six impingers was situated after the filter. Heavy metals and their  
134 compounds in the flue gases were trapped by using a modified standard method.<sup>26</sup> The  
135 first impinger was empty. The second and third impingers were filled with a combined  
136 solution of 5%  $\text{HNO}_3$  and 10%  $\text{H}_2\text{O}_2$  for trapping most of the Pb and Cu and their  
137 compounds from the gases. The fourth and fifth impingers were filled with 4%  
138  $\text{KMnO}_4$  and 10%  $\text{H}_2\text{SO}_4$  to capture trace element. The final impinger was filled with  
139 silica gel to remove the moisture content from the gases.

140



141

142 **Fig 1.** Laboratory apparatus used for cement clinker production.

143



1  
2  
3  
4 144 *2.3. Experimental procedure*

5  
6 145 The phase composition of cement clinkers was controlled by Bogue method<sup>27</sup>  
7  
8 146 (Eq. (1) – (3)). Lime saturation ratio (KH), silica ratio (SM), and alumina ratio (IM)  
9  
10 147 were designed as 0.9, 2.5, and 1.6, respectively. The theoretical mineral composition  
11  
12 148 was calculated to be 56% of tricalcium silicate (C<sub>3</sub>S), 20% of dicalcium silicate (C<sub>2</sub>S),  
13  
14 149 8.6% of calcium aluminate (C<sub>3</sub>A), and 10% of calcium alumino-ferrite (C<sub>4</sub>AF).  
15  
16 150 Cement raw meal with 1.0% of Pb or Cu were prepared and AlCl<sub>3</sub>·6H<sub>2</sub>O was added at  
17  
18 151 percentages of 0.4%, 0.8%, 1.2%, and 1.6% by mass of raw meal. Table 3 lists the  
19  
20  
21  
22  
23 152 formulated mixtures.

24  
25  
26  
27 153 
$$\text{Lime saturation ratio (KH)} = \frac{\text{CaO} - 1.65\text{Al}_2\text{O}_3 - 0.35\text{Fe}_2\text{O}_3}{2.8\text{SiO}_2} \quad (1)$$

28  
29  
30  
31 154 
$$\text{Silica ratio (SM)} = \frac{\text{SiO}_2}{\text{Al}_2\text{O}_3 + \text{Fe}_2\text{O}_3} \quad (2)$$

32  
33  
34  
35 155 
$$\text{Alumina ratio (IM)} = \frac{\text{Al}_2\text{O}_3}{\text{Fe}_2\text{O}_3} \quad (3)$$

36  
37 156 **Table 3**

38  
39 157 Formulated mixtures with Pb, Cu, and AlCl<sub>3</sub>·6H<sub>2</sub>O.

40

ID.	Pb (wt. %)	Cu (wt. %)	AlCl <sub>3</sub> ·6H <sub>2</sub> O (Cl: wt. %)
S <sub>Ref.</sub>	0	0	0
S <sub>Pb</sub>	1.0	0	0
S <sub>Pb-0.4</sub>	1.0	0	0.4
S <sub>Pb-0.8</sub>	1.0	0	0.8
S <sub>Pb-1.2</sub>	1.0	0	1.2
S <sub>Pb-1.6</sub>	1.0	0	1.6
S <sub>Cu</sub>	0	1.0	0
S <sub>Cu-0.4</sub>	0	1.0	0.4
S <sub>Cu-0.8</sub>	0	1.0	0.8
S <sub>Cu-1.2</sub>	0	1.0	1.2
S <sub>Cu-1.6</sub>	0	1.0	1.6

41  
42  
43  
44  
45  
46  
47  
48  
49  
50  
51  
52  
53  
54  
55  
56 158

1  
2  
3  
4 159 The formulated mixtures were thoroughly blended and homogenized in a  
5  
6 160 mechanical planetary mixer. Then each mixture was mixed with 8% of water and  
7  
8 161 pelletized into Ø10×50 mm cylindrical bar under 40 MPa. Each pellet was calcined at  
9  
10 162 900°C, then heated up to 1450°C with a heating rate of 10°C/min, and maintained at  
11  
12 163 1450°C for 30 min. Then the clinkers were cooled quickly in air to the room  
13  
14 164 temperature.  
15  
16  
17  
18  
19  
20

#### 21 166 *2.4. Analytical methods*

22  
23 167 The clinkers were grounded into fine powder. The prepared clinkers were  
24  
25 168 dissolved using an acid mixture of hydrogen peroxide (H<sub>2</sub>O<sub>2</sub>), aqua regia, and  
26  
27 169 hydrogen fluoride (HF) in a volume ratio of 2:5:2 in the microwave digestion system  
28  
29 170 (ZEROM, China). The concentrations of Pb and Cu in the solutions were analyzed by  
30  
31 171 flame atomic absorption spectrometry (AAS, Analytik Jena AG, Germany). The  
32  
33 172 duplicate measurements were carried out for prepared clinkers, and the average values  
34  
35 173 were used to calculate the volatilization percentage according to Eq. (4):  
36  
37  
38  
39

$$40 \quad H = \left\{ 1 - \frac{K}{S/(1 - LOI)} \right\} \times 100\% \quad (4)$$

41  
42 174

43  
44 175 Where, H is the volatilization ratio of Pb or Cu; K (mg/kg) is the content of Pb or Cu  
45  
46 176 in the clinker; S (mg/kg) is the content of Pb or Cu in raw materials; and LOI  
47  
48 177 represents the loss on ignition.  
49  
50

51 178 The distribution of Pb and Cu in the clinker phases was investigated on the  
52  
53 179 polished (Tegramin-25 polishing machine, Struers, Denmark) sections by an electron  
54  
55 180 probe micro-analysis (EPMA-1600, Shimadzu, Japan). The polishing process was as  
56  
57  
58  
59  
60

1  
2  
3  
4 181 follows: sandpaper of #250-mesh for 2min, #800-mesh for 5min, #1200-mesh for  
5  
6 182 10min, #2000-mesh for 15min, and then #4000-mesh for 20min. The measurement  
7  
8 183 was conducted with an acceleration voltage of 15 kV and an electron beam diameter  
9  
10  
11 184 of 1 $\mu$ m. the detection limit of mapping by EPMA for Cu and Pb was about 0.1wt.%.  
12  
13 185 The morphology of the clinkers and element analyses were investigated by scanning  
14  
15 186 electron microscopy (SEM, EVO 18, Carl Zeiss, Germany) equipped with  
16  
17 187 energy-dispersive X-ray spectroscopy (EDS, Oxford Instrument INCAx-sigth  
18  
19 188 EDS-system). SEM/EDS analyses were performed with a 20kV accelerating voltage.  
20  
21  
22  
23 189 The detection limit of EDS for Cu and Pb from the polished samples of clinkers with  
24  
25 190 using long counting times was about 0.05wt.%.

26  
27  
28 191 Thermogravimetric analysis (TG/DTG) was used to investigate temperature  
29  
30 192 conditions and mass changes as well as the effect of  $\text{AlCl}_3 \cdot 6\text{H}_2\text{O}$  on the sintering  
31  
32 193 reactions of the clinker. Thermogravimetric analysis was carried out for the samples  
33  
34 194 of  $S_{\text{ref}}$ ,  $S_{\text{Pb}}$ ,  $S_{\text{Pb-1.6}}$ ,  $S_{\text{Cu}}$  and  $S_{\text{Cu-1.6}}$ . TG and DTG curves were obtained using a  
35  
36 195 NETZSCH STA 449F3 instrument. Runs were conducted using about 20 mg of  
37  
38 196 sample in alumina pans with an air purge gas flow rate of 100 mL/min, equilibration  
39  
40  
41 197 at 30°C for 10-15 min, followed by a heating rate of 10°C/min from 30°C to 1450°C.

42  
43  
44  
45 198 The morphology of mineral phases of the clinkers was observed by a Carl Zeiss  
46  
47 199 GmbH 37081optical microscope (Germany). The samples were cross-sectioned and  
48  
49 200 polished, and the surface of the cross-section was etched by nitric acid dissolved in  
50  
51 201 the alcohol with a volume fraction of 1.0%.

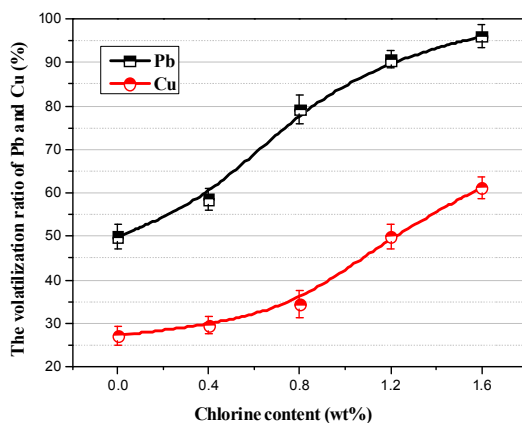
52  
53  
54  
55 202 The qualitative and quantitative mineralogical compositions of the clinkers were  
56  
57  
58  
59  
60

1  
2  
3  
4 203 determined by X-ray diffraction analysis (Bruker D8). This diffractometer is equipped  
5  
6 204 with Cu K $\alpha$  ( $\lambda=1.5406$  Å, 40 kV and 40 mA). A K-value method was adopted to  
7  
8 205 quantify the amount of mineral phases in clinker according to the previous report<sup>28-29</sup>  
9  
10  
11 206 and  $\alpha$ -Al<sub>2</sub>O<sub>3</sub> was used as the internal standard. All patterns were scanned over the  
12  
13 207 range  $5^\circ < 2\theta < 70^\circ$  using a step size of  $0.02^\circ$  and a count time of 0.2 s.  
14  
15  
16 208

### 18 209 3. Results and discussion

#### 20 210 3.1. Volatilization of Pb and Cu with AlCl<sub>3</sub>·6H<sub>2</sub>O

21 211 Figure 2 shows the results obtained for Pb and Cu volatilization. The  
22  
23 212 volatilization ratios of Pb and Cu from the S<sub>Pb</sub> and S<sub>Cu</sub> samples are 49.90% and  
24  
25 213 27.21%, respectively. The volatilization ratios of Pb and Cu increased with increasing  
26  
27 214 AlCl<sub>3</sub>·6H<sub>2</sub>O content. The most significant increase of element volatilization was  
28  
29 215 observed for Pb (46.18%) and Cu (34.04%) with the addition of 1.6% of Cl  
30  
31 216 comparing to the reference sample (Figure 2).  
32  
33  
34  
35  
36

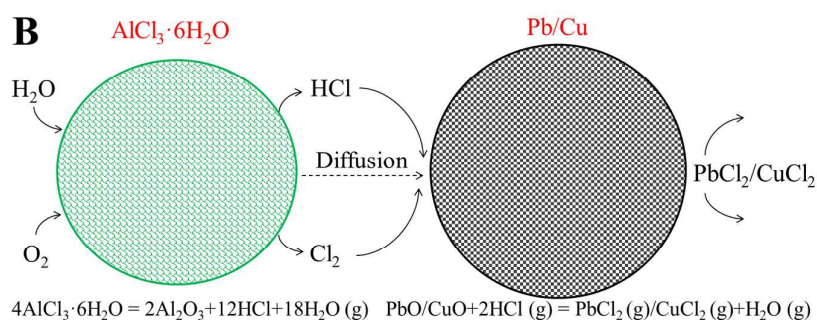
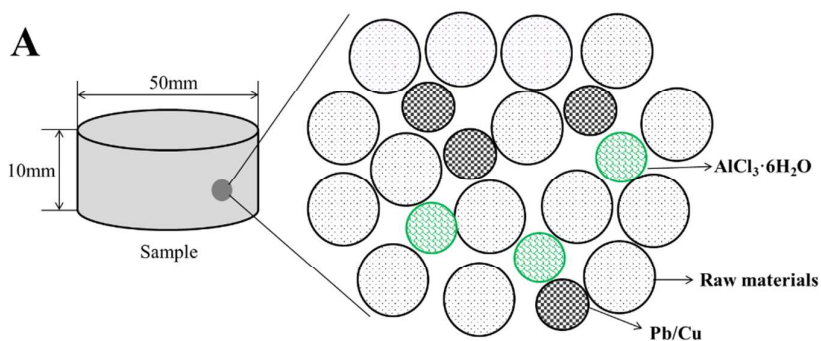


37  
38  
39  
40  
41  
42  
43  
44  
45  
46  
47  
48  
49 217  
50  
51 218 **Fig. 2.** Volatilization of Pb and Cu with AlCl<sub>3</sub>·6H<sub>2</sub>O.  
52  
53  
54 219

55  
56 220 Therefore, the volatilization of Pb and Cu depend strongly on the addition of  
57  
58  
59  
60

221  $\text{AlCl}_3 \cdot 6\text{H}_2\text{O}$ . A schematic diagram of the distribution of Pb or Cu and  $\text{AlCl}_3 \cdot 6\text{H}_2\text{O}$  in a  
 222 pellet and the potential reactions between Pb/Cu and  $\text{AlCl}_3 \cdot 6\text{H}_2\text{O}$  are shown in Figure  
 223 3.  $\text{AlCl}_3 \cdot 6\text{H}_2\text{O}$  release chlorine-containing gas (HCl) with temperature increasing  
 224 according to the reactions in Figure 3.<sup>15</sup> According to Dong et al.,<sup>15</sup> Pb and Cu are  
 225 assumed to be present as oxides at the envisaged temperature (1000°C). The chemical  
 226 reactions show the conversion of PbO and CuO into volatile metal chlorides (Figure  
 227 3).<sup>22,30,31</sup>

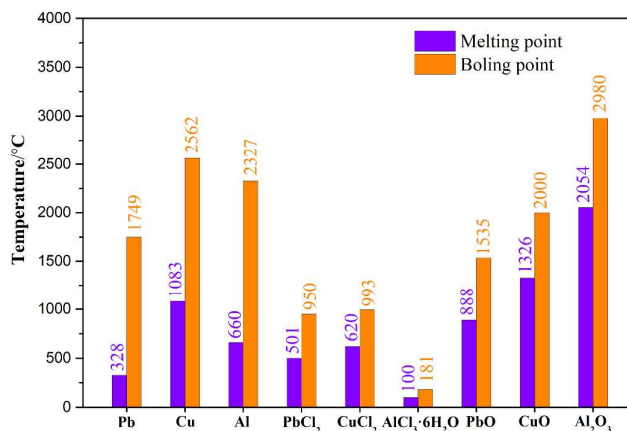
228 The boiling points of PbO and CuO are quite high comparing to the  
 229 correspondent  $\text{PbCl}_2$  and  $\text{CuCl}_2$  (Figure 4). Therefore, the addition of  $\text{AlCl}_3 \cdot 6\text{H}_2\text{O}$  has  
 230 a positive effect on the volatilization of Pb and Cu.



233 **Fig. 3.** Schematic diagram of the distribution of Pb/Cu and  $\text{AlCl}_3 \cdot 6\text{H}_2\text{O}$  in a pellet (A)  
 234 and potential reactions (B).

235

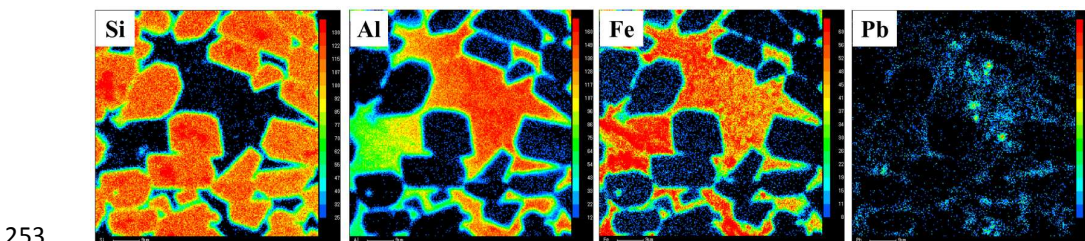
236 Figure 2 shows that Pb is more volatile than Cu at the same content of  
237  $\text{AlCl}_3 \cdot 6\text{H}_2\text{O}$ . The reason is that the melting points and boiling points of PbO and  
238  $\text{PbCl}_2$  are lower than that of CuO and  $\text{CuCl}_2$ , respectively (Figure 4).



239  
240 **Fig. 4.** Melting and boiling points of chemical compounds.

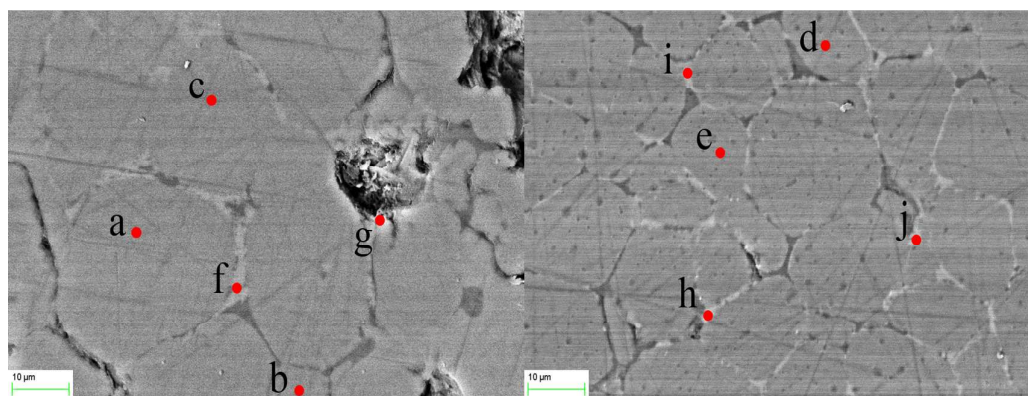
### 241 242 3.2. Solidification of Pb and Cu with $\text{AlCl}_3 \cdot 6\text{H}_2\text{O}$

243 The element distribution maps of Si, Al, Fe, and Pb in the  $\text{S}_{\text{Pb}}$  clinker are shown  
244 in Figure 5. It can be seen that the distributions of Pb, Al and Fe in the clinker are  
245 similar. Thus, Pb was mainly solidified in the interstitial phases of the clinker. Due to  
246 the high volatilization of Pb, especially in the  $\text{S}_{\text{Pb-1.2}}$  and  $\text{S}_{\text{Pb-1.6}}$  clinkers, the  
247 distribution of Pb in the mineral phases is difficult to be confirmed by EPMA.  
248 Therefore, point chemical analysis was carried out to investigate the solidification of  
249 Pb in the  $\text{S}_{\text{Pb-0.8}}$  clinker (Figure 6) and the results are listed in Table 4. Pb was detected  
250 in the interstitial phases but not in the silicate phase of the clinker. Consequently, the  
251 addition of  $\text{AlCl}_3 \cdot 6\text{H}_2\text{O}$  has no effect on the solidified position of Pb.



254 **Fig. 5.** An EPMA maps of distribution of Si, Al, Fe, and Pb in  $S_{Pb}$  clinker.

255



257 **Fig. 6.** Photomicrograph of a backscattered electron image of mineral phases in the  
258  $S_{Pb-0.8}$  sample.

259

260

260 **Table 4**

261 Composition of clinker phases from  $S_{Pb-0.8}$  sample by SEM/EDS (%).

Elements	Points in silicate phase					Points in interstitial phase				
	a	b	c	d	e	f	g	h	i	j
Ca	42.31	44.66	41.73	45.91	40.84	35.20	37.29	35.88	32.84	35.14
O	41.23	38.65	41.95	37.52	42.62	39.98	37.88	37.79	39.86	33.79
Si	14.46	14.77	14.37	14.53	14.26	6.61	5.59	5.89	3.18	2.59
Al	1.29	1.25	1.14	1.21	1.19	9.45	9.37	8.08	13.03	15.29
Fe	0.49	0.46	0.62	0.65	0.19	6.49	7.11	8.14	7.79	8.88
Pb	-	-	-	-	-	0.13	0.10	0.09	0.11	0.14
Others	0.22	0.21	0.19	0.17	0.59	2.14	2.67	4.13	2.71	3.27

262 Note: -, undetected; Error bars: Ca,  $\pm 2.1$ ; O,  $\pm 2.7$ ; Si,  $\pm 1.8$ ; Al,  $\pm 0.12$ ; Fe,  $\pm 0.33$ ; Pb,

263

264

265

266

267

268

269

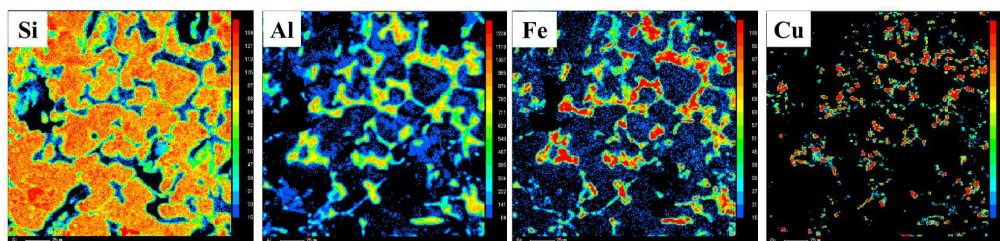
270



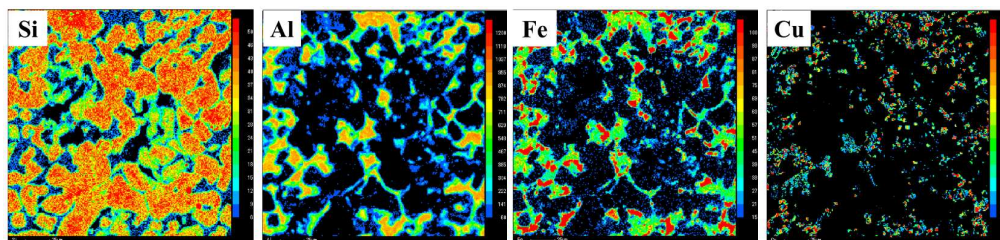
1  
2  
3  
4 263  $\pm 0.14$ .

5  
6 264

7  
8 265 The element distribution maps of Si, Al, Fe, and Cu in the  $S_{Cu}$  and  $S_{Cu-0.8}$  clinkers  
9  
10 266 are shown in Figure 7. Cu was concentrated in the interstitial phases of the clinker  
11  
12 267 (Figure 7A), similar to Pb. The Cu distribution in the clinker phases was not changed  
13  
14 268 after  $AlCl_3 \cdot 6H_2O$  addition. Therefore, the solidified position of Cu was not affected  
15  
16 269 with the presence of  $AlCl_3 \cdot 6H_2O$ .



28  
29 271 (A)



39  
40 273 (B)

41  
42 274 **Fig. 7.** An EPMA maps of distribution of Si, Al, Fe, and Cu in clinkers: A)  $S_{Cu}$ ; B)

43  
44  
45 275  $S_{Cu-0.8}$ .

46  
47 276

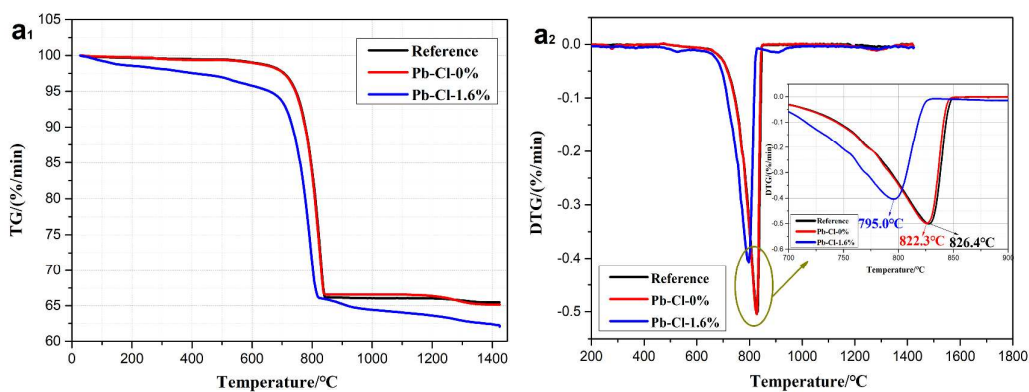
48  
49  
50 277 *3.3. Influence of  $AlCl_3 \cdot 6H_2O$  on the decomposition temperature of limestone*

51  
52 278 The formation of each mineral phases during the process of clinkerization relates  
53  
54 279 to the reactions among CaO, SiO<sub>2</sub>, Al<sub>2</sub>O<sub>3</sub> and Fe<sub>2</sub>O<sub>3</sub>. The reactions are affected by the

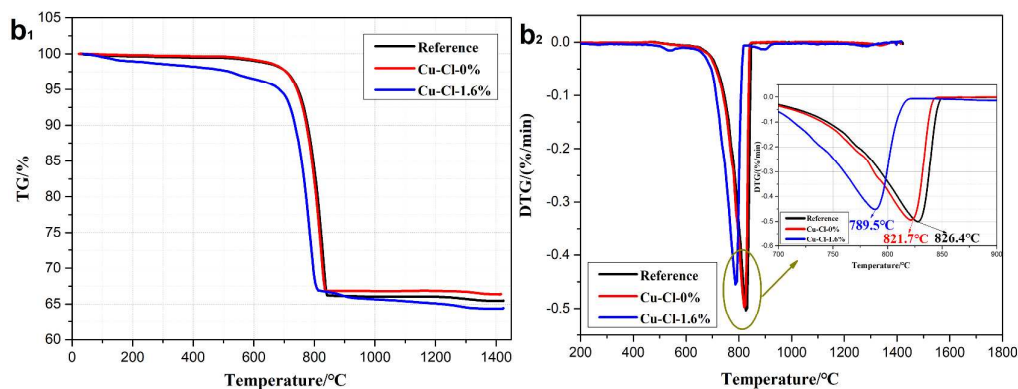


1  
2  
3  
4 280 formation rate of CaO that comes from the decomposition of calcium carbonate (e.g.,  
5  
6 281 limestone).<sup>20</sup> The results from thermogravimetric analysis are shown in Figure 8. The  
7  
8 282 endothermic pick at 826.4°C for the reference sample corresponds to decomposition  
9  
10  
11 283 of CaCO<sub>3</sub>. The decomposition temperature of limestone in the cement mixtures doped  
12  
13 284 with Pb or Cu (e.g., S<sub>Pb</sub> and S<sub>Cu</sub> samples) decreased about 5°C comparing to the S<sub>ref</sub>  
14  
15 285 sample. The addition of 1.6 wt.% of AlCl<sub>3</sub>·6H<sub>2</sub>O (e.g., S<sub>Pb-1.6</sub> and S<sub>Cu-1.6</sub> samples) lead  
16  
17 286 to decrease of the CaCO<sub>3</sub> decomposition temperature significantly (about 30°C lower  
18  
19  
20 287 than for the reference sample). AlCl<sub>3</sub>·6H<sub>2</sub>O played the role as a mineralizer  
21  
22  
23 288 accelerating the decomposition of CaCO<sub>3</sub>. According to other research,<sup>20</sup> the  
24  
25 289 incorporation of chlorine in the cement raw meal could promote the decomposition of  
26  
27  
28 290 CaCO<sub>3</sub>, decrease temperature of the first liquid phase formation, increase the amount  
29  
30  
31 291 of the melt, and accelerate the rate of the reactions occurring in the solid state.

292



293



294

295 **Fig. 8.** TG-DTG curves of the following cement mixtures: a<sub>1</sub>) TG curves of  $S_{ref}$ ,  $S_{Pb}$ 296 and  $S_{Pb-1.6}$ ; a<sub>2</sub>) DTG curves of  $S_{ref}$ ,  $S_{Pb}$  and  $S_{Pb-1.6}$ ; b<sub>1</sub>) TG curves of  $S_{ref}$ ,  $S_{Cu}$  and  $S_{Cu-1.6}$ ;297 b<sub>2</sub>) DTG curves  $S_{ref}$ ,  $S_{Cu}$  and  $S_{Cu-1.6}$ .

298

299 

### 3.4. Influence of $AlCl_3 \cdot 6H_2O$ on the crystal sizes of alite and belite

300 The optical photomicrographs of the  $S_{ref}$ ,  $S_{Pb}$ ,  $S_{Pb-1.6}$ ,  $S_{Cu}$ , and  $S_{Cu-1.6}$  clinkers are

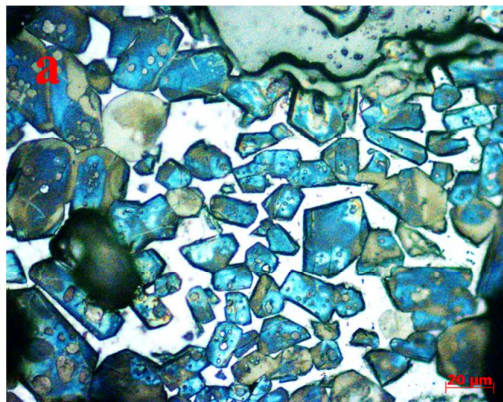
301 given in Figure 9. All investigated clinkers consist of main silicate minerals such as

302 alite ( $C_3S$ ), belite ( $C_2S$ ), and interstitial phases including matrix of calcium aluminate303 ( $C_3A$ ) and calcium aluminoferrite ( $C_4AF$ ). The fifty typical micrographs were taken

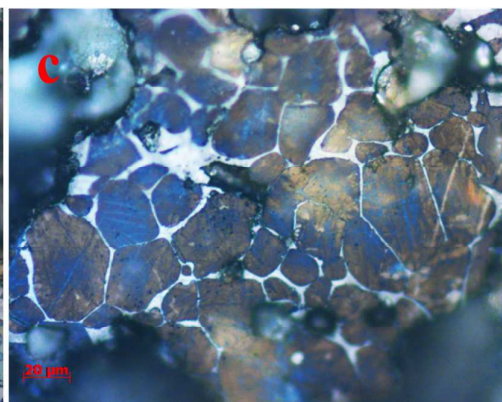
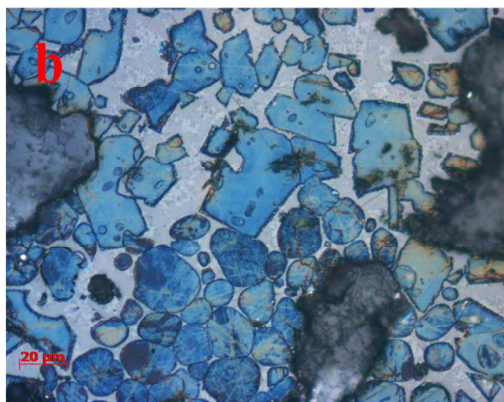
304 for each sample in order to estimate the crystal sizes of alite and belite (Table 5). The

305 average crystal sizes of alite and belite in the  $S_{ref}$  clinker are in the range of 15-25  $\mu m$ 306 and 10-20  $\mu m$ , respectively. There were not visible changes in the alite and belite307 crystal sizes for the  $S_{Pb}$  and  $S_{Cu}$  samples. However, the crystal sizes of alite and belite308 in the  $S_{Pb-1.6}$  and  $S_{Cu-1.6}$  clinkers increased considerably comparing to the  $S_{Pb}$ ,  $S_{Cu}$ , and309  $S_{ref}$  samples.

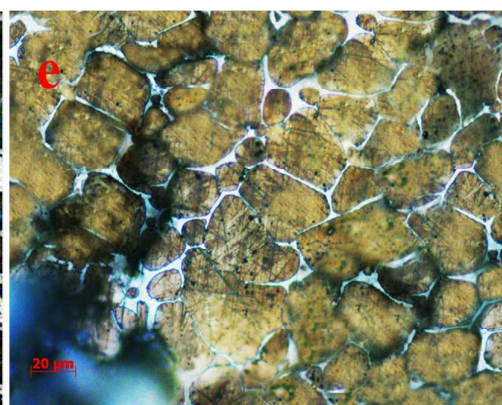
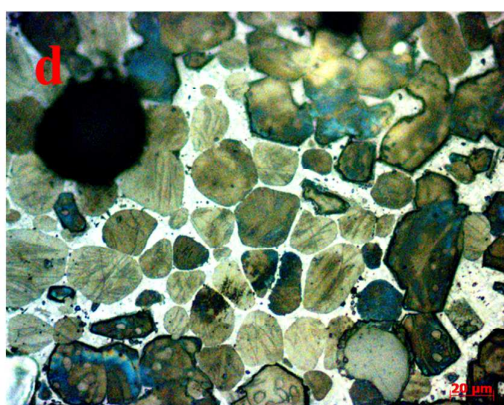
310



311



312



313 **Fig. 9.** Optical photomicrographs for the clinkers: (a)  $S_{Ref.}$ ; (b)  $S_{Pb}$ ; (c)  $S_{Pb-1.6}$ ; (d)  $S_{Cu}$ ;

314

(e)  $S_{Cu-1.6}$ .

315

316 **Table 5**

317 Size and shape of alite and belite crystals in clinkers

ID.	Alite	Belite
-----	-------	--------

	Size ( $\mu\text{m}$ )	Shape	Size ( $\mu\text{m}$ )	Shape
$S_{\text{ref}}$	15-25	Angular, elongated, prismatic	10-20	Small, roundish
$S_{\text{Pb}}$	15-30	Prismatic, angular	10-25	Small, roundish
$S_{\text{Pb-1.6}}$	30-50	Large, compact, prismatic, angular	20-30	Large, round, compact
$S_{\text{Cu}}$	15-30	Prismatic, angular	10-25	Small, roundish
$S_{\text{Cu-1.6}}$	30-50	Large, compact, prismatic, angular	20-30	Large, round, compact

318

319 According to Taylor et al.,<sup>27</sup> Kacimi et al.<sup>32</sup> and Wang et al.,<sup>33</sup> chlorine dissolved  
 320 in the melt can affect the acid-base equilibrium  $[\text{MeO}_4]^{5-} \leftrightarrow [\text{MeO}_6]^{9-}$  of the  
 321 amphoteric elements ( $\text{Al}^{3+}$  and  $\text{Fe}^{3+}$ ). The displacement of this reaction to the left  
 322 favors the formation of a network built from  $[\text{MeO}_4]^{5-}$  and silicon tetrahedra that leads  
 323 to the increase of the melt viscosity, while  $[\text{MeO}_6]^{9-}$  is more mobile and promotes the  
 324 decrease of the viscosity surface tension of the melt, and then promote the silicate  
 325 crystals (e.g.,  $\text{C}_3\text{S}$  and  $\text{C}_2\text{S}$ ) formation and growth.

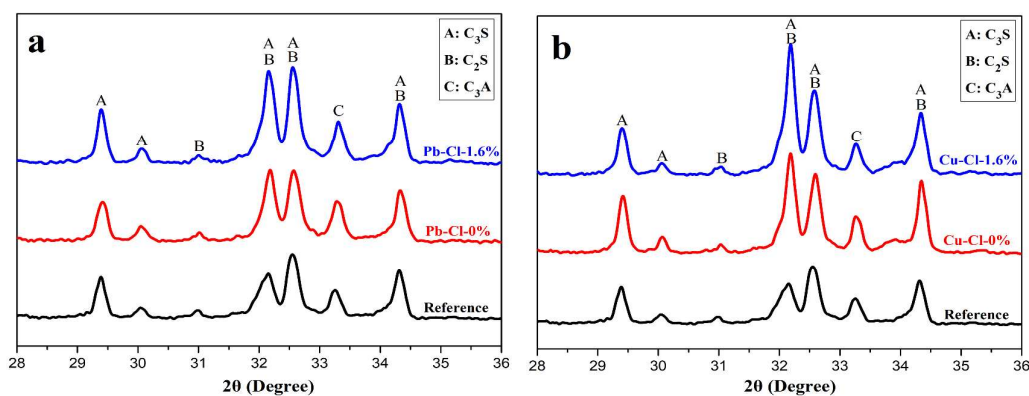
326

### 327 3.5. Influence of $\text{AlCl}_3 \cdot 6\text{H}_2\text{O}$ on the mineral composition of the clinker

328 X-ray diffraction is a reliable and precise method to quantify the relative phase  
 329 content in the Portland cement clinker.<sup>34</sup> The content of silicate and interstitial phases  
 330 of the clinkers were determined by quantitative XRD analysis and the results are  
 331 listed in Figure 10 and Table 6. The content of silicate phase is 79.2% with 54.2%  $\text{C}_3\text{S}$   
 332 and 25.0%  $\text{C}_2\text{S}$  for the reference sample, which is consistent with the calculated  
 333 mineral composition by Bogue method. For the samples of  $S_{\text{Pb}}$  and  $S_{\text{Cu}}$ , the main  
 334 peaks intensity of  $\text{C}_3\text{S}$  in the XRD patterns (Figure 10) increased a little bit and the  
 335 content of  $\text{C}_3\text{S}$  is slightly higher but contents of  $\text{C}_2\text{S}$ ,  $\text{C}_3\text{A}$ , and  $\text{C}_4\text{AF}$  are slightly

336 lower than for  $S_{\text{Ref}}$ . Addition of 1.6 wt.% of  $\text{AlCl}_3 \cdot 6\text{H}_2\text{O}$  leads to significant increase  
 337 the main peaks intensity and content of  $\text{C}_3\text{S}$ , about 10 wt.% higher than for reference  
 338 clinker. Amount of  $\text{C}_2\text{S}$  decrease in 1.65 wt.% for the  $S_{\text{Pb-1.6}}$  clinker and in 2.68 wt.%  
 339 for the  $S_{\text{Cu-1.6}}$  clinker comparing to  $S_{\text{Ref}}$ . The content of  $\text{C}_3\text{A}$  and  $\text{C}_4\text{AF}$  (interstitial  
 340 phases) decreased considerably (about 8 wt.%) for both  $S_{\text{Pb-1.6}}$  and  $S_{\text{Cu-1.6}}$  clinkers  
 341 (Table 6). Combined with the results in Section 3.2, Pb and Cu were concentrated in  
 342 interstitial phases of the clinker and being not affected by the addition of  $\text{AlCl}_3 \cdot 6\text{H}_2\text{O}$ .  
 343 It can be obtained that chlorine decreased the ability of clinker to solidify Pb and Cu  
 344 during clinkerization. Accordingly, to increase the solidification of Cu and Pb in  
 345 clinker, the content of interstitial phases in clinker should be increased properly  
 346 through adjusting the KH, SM, and IM by Bogue method<sup>26</sup> during the co-processing  
 347 of chlorine-contained solid waste in cement kiln.

348



349

350 **Fig. 9.** XRD patterns of clinker. a)  $S_{\text{ref}}$ ,  $S_{\text{Pb}}$  and  $S_{\text{Pb-1.6}}$ ; b)  $S_{\text{ref}}$ ,  $S_{\text{Cu}}$  and  $S_{\text{Cu-1.6}}$ .

351

### 352 Table 6

353 Mineral composition of the clinkers, wt.%

354

355

356

357

358

359

360

ID.	Silicate phase		Interstitial phase		
	C <sub>3</sub> S	C <sub>2</sub> S	C <sub>3</sub> A	C <sub>4</sub> AF	Others
S <sub>Ref</sub>	54.2±0.8	25.0±0.6	9.6±0.3	8.3±0.5	2.8±0.2
S <sub>Pb</sub>	56.4±0.6	23.5±0.7	9.4±0.2	8.2±0.4	2.4±0.3
S <sub>Pb-1.6</sub>	64.9±0.4	23.4±0.3	5.0±0.4	4.6±0.5	2.2±0.1
S <sub>Cu</sub>	55.8±0.5	24.1±0.4	8.9±0.6	8.0±0.6	3.2±0.3
S <sub>Cu-1.6</sub>	64.7±0.9	22.3±0.2	3.8±0.2	6.2±0.8	3.0±0.4

354

355 **4. Conclusions**

356 The relationships among chlorine, volatilization and solidification of Cu/Pb, and  
 357 mineral phases of the clinker during clinkerization were investigated and discussed in  
 358 this work. The main conclusions can be summarized as follow:

- 359 • Chlorine has a significant effect on the volatilization of Pb and Cu in  
 360 clinkerization. The volatilization ratios of Pb and Cu increased up to 46.18% and  
 361 34.04%, respectively, with increasing AlCl<sub>3</sub>·6H<sub>2</sub>O content up to 1.6%. comparing  
 362 to the cement mixtures without AlCl<sub>3</sub>·6H<sub>2</sub>O addition (Pb and Cu volatilisations  
 363 are 49.90% and 27.21%, respectively).
- 364 • Pb and Cu were concentrated in the interstitial phases of the clinker and being not  
 365 affected by the addition of chlorine.
- 366 • The crystal formation and growth of alite and belite were promoted by chlorine.  
 367 The crystal sizes of alite and belite increased about 100% and 70%, respectively,  
 368 when the content of chlorine was 1.6%. The content of C<sub>3</sub>S increased about 10  
 369 wt.% with the corresponding content of interstitial phases decreased about 8 wt.%  
 370 during clinkerization with the addition of 1.6% Cl.
- 371 • Chlorine decreased the ability of clinker to solidify Pb and Cu by decreasing the



1  
2  
3  
4 372 content of interstitial phases in clinkerization.  
5

6 373 However, there are some experiments and questions that deserve to be done  
7  
8 374 and discussed in the future. Firstly, determination of the effects of chlorine on the  
9  
10 375 volatilization of Pb and Cu in this study was at the temperature of 1450□. Indeed,  
11  
12 376 the cement raw meal will undergo different temperature ranges during the  
13  
14 377 process of being sintered to clinker. Therefore, the study of the chlorine effect to  
15  
16 378 the volatilization of Pb and Cu at different temperatures during clinkerization is  
17  
18 379 required. Secondly, the effect of chlorine on the volatilization of Pb and Cu may  
19  
20 380 be different, if Pb and Cu exist simultaneously due to their possible competitive  
21  
22 381 effects. Therefore, it is interesting to investigate the effect of chlorine on the  
23  
24 382 volatilization of heavy metals from mono-elemental system to multi-elemental  
25  
26 383 system in the future.  
27  
28  
29  
30  
31  
32  
33  
34

### 35 385 **Acknowledgements**

36  
37 386 This work was supported by the National Natural Science Foundation of China  
38  
39 387 (NSFC, No. 5141101056) and Guangdong science and Technology Department  
40  
41 388 (2014B020216002).  
42  
43  
44

### 45 389 46 47 390 **References**

- 48  
49  
50 391 (1) Zhang, S.; Ernst, W.; Wina C. Evaluating co-benefits of energy efficiency and air  
51  
52 392 pollution abatement in China's cement industry. *Appl. Energ.* 2015, 147, 192-213.  
53  
54  
55 393 (2) China Environmental State Bulletin: 2017.  
56  
57  
58  
59  
60

- 1  
2  
3  
4 394 (3) Dong, J.; Chi, Y.; Tang, Y.; Wang, F.; Huang, Q. Combined Life Cycle  
5  
6 395 Environmental and Exergetic Assessment of Four Typical Sewage Sludge Treatment  
7  
8 396 Techniques in China. *Energy Fuels*. 2014, 28, 2114–2122.
- 9  
10  
11 397 (4) Rahman, A.; Rasul, M. G.; Khan, M. M. K.; Sharma, S. Impact of alternative fuels  
12  
13 398 on the cement manufacturing plant performance: an overview. *Procedia Eng.* 2013, 56,  
14  
15 399 393–400.
- 16  
17  
18 400 (5) Maria del, M. C. M.; Linda, K. N.; Flemming, J. F.; Peter, G.; Kim, D. J. Review:  
19  
20 401 Circulation of Inorganic Elements in Combustion of Alternative Fuels in Cement  
21  
22 402 Plants. *Energy Fuels*. 2015, 29, 4076–4099.
- 23  
24  
25 403 (6) Qiu, Q.; Jiang, X.; Lv, G.; Lu, S.; Ni, M. Stabilization of Heavy Metals in  
26  
27 404 Municipal Solid Waste Incineration Fly Ash in Circulating Fluidized Bed by  
28  
29 405 Microwave-Assisted Hydrothermal Treatment with Additives. *Energy Fuels*. 2016, 30,  
30  
31 406 7588–7595.
- 32  
33  
34  
35 407 (7) Chanaka, U. W. D.; Andrei, V.; Apostolos, G.; Grzegorz, L.; Victor W. C.;  
36  
37 408 Teik-Thye, L. Fate and distribution of heavy metals during thermal processing of  
38  
39 409 sewage sludge. *Fuel*. 2018, 226, 721–744.
- 40  
41  
42 410 (8) Mu, Y.; Amirhomayoun, S.; Takayuki, S. Utilization of waste natural fishbone for  
43  
44 411 heavy metal stabilization in municipal solid waste incineration fly ash. *J. Clean. Prod.*  
45  
46 412 2018, 172, 3111–3118.
- 47  
48  
49  
50 413 (9) Zain, A. S. B.; Li, R.; Li, Y.; Gao, H.; Teerawat, S.; Teng, W.; Sunel, K.; Liang, Z.  
51  
52 414 New advancement perspectives of chloride additives on enhanced heavy metals  
53  
54 415 removal and phosphorus fixation during thermal processing of sewage sludge. *J.*



- 1  
2  
3  
4 416 Clean. Prod. 2018, 188, 185–194.  
5  
6 417 (10) Ke, C.; Ma, X.; Tang, Y.; Zheng, W.; Wu, Z. The volatilization of heavy metals  
7  
8 418 during co-combustion of food waste and polyvinyl chloride in air and carbon  
9  
10 419 dioxide/oxygen atmosphere. *Bioresource Technol.* 2017, 244, 1024-1030.  
11  
12  
13 420 (11) Krzysztof, F.; Agnieszka, R.; Anna, G.; Malgorzata, J. K. The presence of  
14  
15 421 contaminations in sewage sludge–The current situation. *J. Environ. Manage.* 2017, 203,  
16  
17 422 1126–1136.  
18  
19  
20 423 (12) Quina, M. J.; Bontempi, E.; Bogush, A.; Schlumberger, S.; Weibel, G.; Braga, R.;  
21  
22 424 Funari, V.; Hyks, J.; Rasmussen, E.; Lederer, J. Technologies for the management of  
23  
24 425 MSW incineration ashes from gas cleaning: new perspectives on recovery of  
25  
26 426 secondary raw materials and circular economy. *Sci. Total Environ.* 2018, 635, 526–  
27  
28 427 542.  
29  
30  
31  
32 428 (13) Yan, D.; Karstensen, K. H.; Huang, Q.; Wang, Q.; Cai, M. Coprocessing of  
33  
34 429 industrial and hazardous wastes in cement kilns: A review of current status and future  
35  
36 430 needs in China. *Environ. Eng. Sci.* 2010, 27, 37–45.  
37  
38  
39  
40 431 (14) Gupta, R. K.; Majumdar, D.; Trivedi, J. V.; Bhanarkar, A. D. Particulate matter  
41  
42 432 and elemental emissions from a cement kiln. *Fuel Process. Technol.* 2012, 104, 343–  
43  
44 433 351.  
45  
46  
47 434 (15) Dong, J.; Chi, Y.; Tang, Y.; Ni, M.; Nzihou, A.; Weiss, H. E.; Huang, Q.  
48  
49 435 Partitioning of Heavy Metals in Municipal Solid Waste Pyrolysis, Gasification, and  
50  
51 436 Incineration. *Energy Fuels.* 2015, 29, 7516–7525.  
52  
53  
54  
55 437 (16) Yu, J.; Sun, L.; Ma, C.; Qiao, Y.; Xiang, J.; Hu, S.; Yao, H. Mechanism on heavy  
56  
57  
58  
59  
60

- 1  
2  
3  
4 438 metals vaporization from municipal solid waste fly ash by  $\text{MgCl}_2 \cdot 6\text{H}_2\text{O}$ . Waste  
5  
6 439 Manage. 2016, 49, 124–130.  
7  
8 440 (17) Nowak, B.; Pessl, A.; Aschenbrenner, P.; Szentannai, P.; Mattenberger, H.;  
9  
10 441 Rechberger, H.; Hermann, L.; Winter, F. Heavy metal removal from municipal solid  
11  
12 442 waste fly ash by chlorination and thermal treatment. J. Hazard. Mater. 2010, 179,  
13  
14 443 323–331.  
15  
16 444 (18) Nowak, B.; Rocha, F.S.; Aschenbrenner, P.; Rechberger, H.; Winter, F. Heavy  
17  
18 445 metal removal from MSW fly ash by means of chlorination and thermal treatment:  
19  
20 446 Influence of the chloride type. Chem. Eng. J. 2012, 179, 178–185.  
21  
22 447 (19) Jawed, I.; Skalny, J. Alkalies in cement: a review. Cem. Concr. Res. 1977, 7,  
23  
24 448 719–730.  
25  
26 449 (20) Kolovos, K.; Tsvivilis, S.; Kakali, G. The effect of foreign ions on the reactivity of  
27  
28 450 the  $\text{CaO-SiO}_2\text{-Al}_2\text{O}_3\text{-Fe}_2\text{O}_3$  system. Cem. Concr. Res. 2002, 32, 463–469.  
29  
30 451 (21) Lu, Q.; Dong, W.; Wang, H.; Wang, X. A Novel Way to Synthesize Yttrium  
31  
32 452 Aluminum Garnet from Metal-Inorganic Precursors, J. Am. Ceram. Soc. 2002, 85,  
33  
34 453 490–492.  
35  
36 454 (22) Yu, S.; Zhang, B.; Wei, J.; Zhang, T.; Yu, Q.; Zhang, W.; Effects of chlorine on  
37  
38 455 the volatilization of heavy metals during the co-combustion of sewage sludge. Waste  
39  
40 456 Manage. 2017, 62, 204–210.  
41  
42 457 (23) Jiang, Y.; Lin, T. C.; Shi, C.; Pan, S. Characteristics of steel slags and their use in  
43  
44 458 cement and concrete—A review. Resour. Conserv. Recy. 2018, 136, 187–197.  
45  
46 459 (24) Ludwig, H. M.; Zhang, W. Research review of cement clinker chemistry. Cem.  
47  
48  
49  
50  
51  
52  
53  
54  
55  
56  
57  
58  
59  
60

- 1  
2  
3  
4 460 Concr. Res. 2015, 78, 24–37.
- 5  
6 461 (25) Fukuda, K.; Matsunaga K.; Bessho, T.; Yoshida, H. Melt Differentiation Induced  
7  
8 462 by Zonal Structure Formation of Calcium Aluminoferrite in a CaO-SiO<sub>2</sub>-Al<sub>2</sub>O<sub>3</sub>-Fe<sub>2</sub>O<sub>3</sub>  
9  
10 463 Pseudoquaternary System. *J. Am. Ceram. Soc.* 2005, 88, 954–962.
- 11  
12  
13 464 (26) U.S. Environmental Protection Agency (USEPA), Method 29–Determination of  
14  
15 465 Metal Emissions from Stationary Sources, Office of Air Quality Planning and  
16  
17 466 Standards, Washington, D.C, 1996.
- 18  
19  
20 467 (27) H. F. W. Taylor, *Cement Chemistry*, second ed. Thomas Telford, New York, 1997.
- 21  
22  
23 468 (28) Li, J.; Yu, Q.; Wei, J.; Zhang, T. Structural characteristics and hydration kinetics  
24  
25 469 of modified steel slag. *Cem. Concr. Res.* 2011, 41, 324–329.
- 26  
27  
28 470 (29) Guilherme, A. C.; Thais, L. T. S.; Ana Paula, B. R.; Adenilson, O. S.; Lisandro, P.  
29  
30 471 C. On the quantitative phase analysis and amorphous content of triacylglycerols  
31  
32 472 materials by X-ray rietveld method. *Chem. Phys. Lipids*. Available online, 2018.
- 33  
34  
35 473 (30) Chan, C.; Jia, C. Q.; Graydon, J. W.; Kirk, D. W. The behaviour of selected  
36  
37 474 heavy metals in MSW incineration electrostatic precipitator ash during roasting with  
38  
39 475 chlorination agents. *J. Hazard. Mater.* 1996, 50, 1–13.
- 40  
41  
42 476 (31) Liu, J.; Chen, J.; Huang, L. Heavy metal removal from MSS fly ash by thermal  
43  
44 477 and chlorination treatments. *Sci. Rep.* 2015, Article number: 17270.
- 45  
46  
47 478 (32) Kacimi, L.; Simon-Masseron, A.; Ghomari, A.; Derriche, Z. Reduction of  
48  
49 479 clinkerization temperature by using phosphogypsum. *J. Hazard. Mater.* 2006, 37, 129–  
50  
51 480 137.
- 52  
53  
54 481 (33) Wang, F.; Shang, D.; Wang, M.; Hu, S.; Li, Y. Incorporation and substitution  
55  
56  
57  
58  
59  
60

- 1  
2  
3  
4 482 mechanism of cadmium in cement clinker. *J. Clean. Prod.* 2016, 112, 2292–2299.  
5  
6 483 (34) Witte, M. Lesch, C. On the improvement of measurement accuracy of retained  
7  
8 484 austenite in steel with X-ray diffraction. *Mater. Charact.* 2018, 139, 111–115.  
9  
10  
11  
12  
13  
14  
15  
16  
17  
18  
19  
20  
21  
22  
23  
24  
25  
26  
27  
28  
29  
30  
31  
32  
33  
34  
35  
36  
37  
38  
39  
40  
41  
42  
43  
44  
45  
46  
47  
48  
49  
50  
51  
52  
53  
54  
55  
56  
57  
58  
59  
60